Anomalous three-dimensional symmetries of solar-wind plasma

A. Bershadskii
ICAR, P. O. Box 31155, Jerusalem 91000, Israel

(Received 18 April 2002; revised manuscript received 24 June 2002; published 15 October 2002)

An example of a combination of Kolmogorov three-dimensional properties with Alfvén two-dimensional properties in solar-wind plasma is given using recent data obtained with the Advanced Composition Explorer satellite at the L1 libration point. Both spectral and moments scaling analyses are used to demonstrate the possibility of such a combination. Two-decade scaling and the large number of the scaling exponents under consideration indicate the robustness of this observation.

DOI: 10.1103/PhysRevE.66.046410 PACS number(s): 95.30.Qd, 96.50.Ci, 52.30.Cv

Solar wind is an actively evolving turbulent magnetofluid, stirred by solar rotation and shears between and within streams. The Alfvén nature of the solar wind originates in the solar corona, but is modified and reduced in the heliosphere by velocity shears. It is of fundamental importance to learn the nature of three-dimensional (3D) symmetries of the solar-wind fluctuations because it is the three-dimensional properties that determine how both solar energetic particles and galactic cosmic rays propagate throughout the heliosphere; determining, e.g., whether or not solar energetic particles from flares and coronal mass ejections will impact the Earth. However, the symmetries of the solar-wind fluctuations are still an open problem (see, for recent reviews Refs. [1,2]). How much of the observed population of fluctuations with wave vectors highly oblique to the mean magnetic field originates in the corona and how much is generated *in situ* by velocity shear? This distinction is particularly important because quasi-two-dimensional turbulence originating in the solar corona will not pitch-angle scatter the energetic particles. When the quasi-two-dimensional component of solar-wind fluctuations was first described [3], it was assumed to have arisen due to the effect of the background magnetic field (see, for corresponding numerical simulations, in Refs. [4,5]). There also exist other mechanisms that can produce a large component of wave vectors peaked orthogonal to the background magnetic field. These include velocity shear, pressure-balanced structures, and quasistatic conditions in the solar corona. At 1 a.u. the solar wind consists of a mix of Alfvén fluctuations, convected structures, streams of various amplitudes, and propagating compressive structures. All of these interact after leaving the solar corona. At periods shorter than the solar rotation period, the interaction between fast and slow solar-wind streams drives nonlinear couplings, producing a flow of energy in wave number space from large to small scales, which is ultimately dissipated by kinetic effects. Although even small amplitude waves will be distorted by velocity shear or by density gradients including linear mode coupling, both simulations and observations indicate that velocity shears in the solar wind drive nonlinear interactions that reduce the Alfvén nature of the turbulence.

The spherical expansion influences the development of a turbulent cascade for parallel propagating fluctuations [6]—the effect on nearly two dimensional fluctuations is similar [7]. Although a turbulent cascade can be sustained in a spherically expanding magnetofluid, there is no known theoretical reason for the slope of the resulting power spectra to approach the Kolmogorov value of $-5/3$ since the medium is compressible and not isotropic. However, in solar-wind power spectra of the magnetic field or velocity fluctuations often contained an ''inertial'' range with a slope of approximately $-5/3$, which is the value predicted and observed for isotropic incompressible Navier-Stokes fluid turbulence [8]. The early solar-wind observations could not distinguish clearly between the Kolmogorov $-5/3$ slope and the Iroshnikov $-3/2$ slope predicted for ideal isotropic incompressible magnetohydrodynamic (MHD) turbulence. The first $-5/3$ wave number solar-wind magnetic energy spectrum measurement was reported in Ref. [9]. The next two decades saw strenuous assertion of the $-3/2$ exponent. More recent works indicate that the spectral slope is more often $-5/3$. While it could be argued that the solar wind is approximately incompressible, at least in regions devoid of shock waves and corotating interaction regions, the presence of a relatively strong magnetic field indicates that isotropy is not a good assumption, and one might therefore expect that the Iroshnikov prediction of the $-3/2$ for the Alfvén turbulence would be observed. The first demonstration of the tendency towards anisotropy in the presence of a nonzero mean magnetic field was a numerical simulation due to the authors of Ref. [10]. The first suggestion of a $-5/3$ 2D MHD isotropic spectrum in two directions perpendicular to the mean magnetic field, simultaneously with a non-power-law falloff, dominated by slower transfer in the parallel direction, was given by Montgomery [11].

The simplest interpretation of the strong Alfvén nature of solar-wind fluctuations is that they are both planar and parallel propagating. Such waves pitch-angle scatter charged particles efficiently as they propagate along the background magnetic field, but allow for relatively little transverse diffusion across the magnetic field. The first indication that this simple point of view was inadequate was an analysis [3] of nearly two years of magnetometer data from the ISEE-3 spacecraft which accumulated solar-wind magnetic field data nearly continuously at the Earth's libration point. By organizing the magnetometer data into statistically stationary subsets of what they assumed to be a single ensemble of the interplanetary magnetic field, the authors of Ref. [3] succeeded in constructing a two-dimensional correlation function of the interplanetary magnetic field (IMF) fluctuations. The correlation function revealed the existence of a second

component, in addition to the expected Alfvén fluctuations, that had the symmetry of quasi-two-dimensional structures. More precisely, the results indicate that the ensemble is dominated by two populations: fluctuations with large correlation lengths perpendicular to the mean magnetic field $\mathbf{B}_0$ and fluctuations with large correlation lengths parallel to $\mathbf{B}_0$. Subsequent analysis suggested that nearly 80% of the interplanetary turbulence might consist of fluctuations with $\mathbf{k}$ perpendicular to $\mathbf{B_0}$ [12]. In contrast, other works suggest that the non-Alfvén component of the fluctuations involves ''structures'' with magnetic fluctuations parallel to $\mathbf{B}_0$ [13,14]. In paper [15] the role of small velocity shears in generating a significant population of fluctuations with wave numbers nearly orthogonal to $\mathbf{B}_0$ was also analyzed.

Though the comprehensive analysis of the two year magnetometer data performed in Ref. [3] gives a general statistical picture of the fluctuations population it seems to be useful to look at an individual ''element'' of this population with a certain three-dimensional symmetry and in its own characteristic time scales.

For this purpose we will first use one-day (January 30, 2002) data set obtained from a ACE (Advanced Composition Explorer) satellite magnetometer. The reason for such time frames is the intrinsic *scaling* properties of the ''individual'' fluctuations (see below). In order to get away from the effects of the Earth's magnetic field, the ACE spacecraft orbits at the L1 libration point which is a point of Earth-Sun gravitational equilibrium about 1.5×10^6 km from Earth and 148.5×10^6 km from the sun. With a semimajor axis of approximately 200 000 km the elliptical orbit affords ACE a prime view of the Sun and the galactic regions beyond. ACE stays in a relatively constant position with respect to the Earth as the Earth revolves around the Sun. The two magnetometers on ACE are wide-range (±0.004 to 65536 nT) triaxial fluxgate magnetometers. They are mounted remotely from the spacecraft on separate booms in order to reduce any effect of magnetics from the spacecraft and other instruments. They measure the amplitude and direction of the interplanetary magnetic field thirty times per second. We then use 1-min averaging data. We use the magnetometer values in so-called GSM (geocentric solar magnetospheric) coordinates. The GSM system of coordinates has its x axis from the Earth to the Sun. The Y axis is defined to be perpendicular to the Earth's magnetic dipole so that the x-z plane contains the dipole axis.

Then we consider analogous data for an additional six-day period: 31 January–5 February 2002, but now with 5-min averaging.

Figure 1 shows energy spectra of the B_x component of the measured magnetic field (measured in nT). The straight line (the best fit) is drawn to indicate scaling law dependence (in the log-log scales). The line slope -1.7 ± 0.1 indicates Kolmogorov-like scaling $-5/3$.

To relate the observed slope strictly to the Kolmogorov one we need the Taylor frozen-flow hypothesis: substitution of frequency for wave number [8]. To justify the use of the Taylor hypothesis one needs information on the local velocity field, which unfortunately is not available to us. To explore this observation further we have calculated the intermittency exponents ζ_p extracted from the data in the scaling assumption

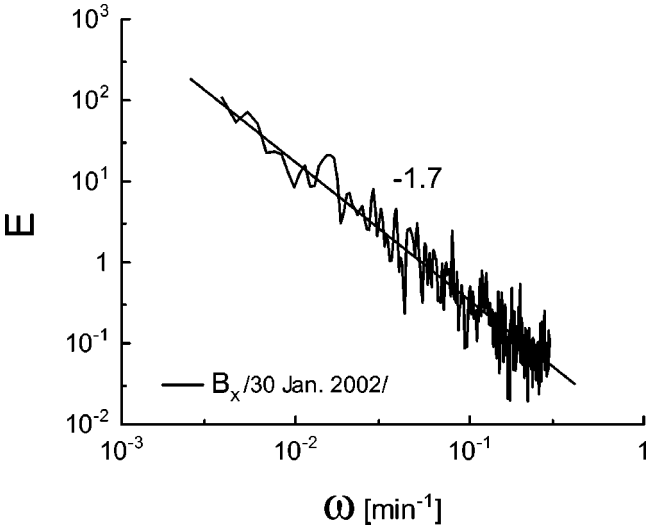

FIG. 1. Energy spectra of the B_x component of the IMF (measured in nT). The straight line (the best fit) is drawn to indicate scaling law dependence (in the log-log scales). The line slope -1.7 ± 0.1 indicates Kolmogorov-like scaling $-5/3$.

$$\langle|\Delta B_x|^p\rangle\sim\Delta t^{\zeta_p}, \tag{1}$$

where

$$\Delta B_x = B_x(t+\Delta t)-B_x(t). \tag{2}$$

Figure 2 shows $\log_{10}\langle|\Delta B_x|^p\rangle$ versus $\log_{10}\Delta t$ for first five moments ($p=1,2,\ldots,5$) and the straight lines (the best fit) are drawn to indicate scaling (1). The magnetic field is measured in the units 10 nT here. The most significant observation here is that

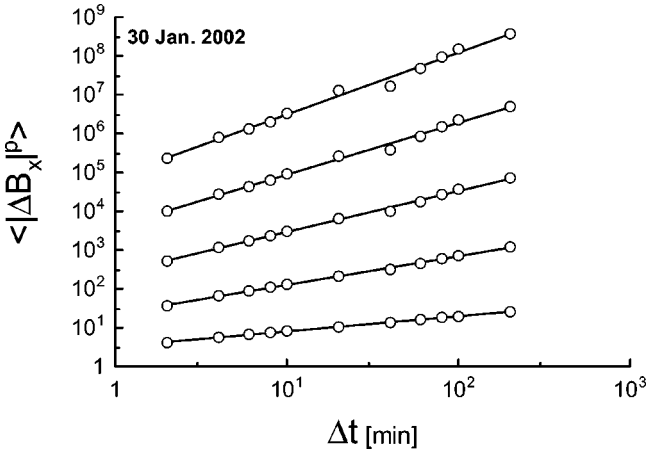

FIG. 2. $\log_{10}\langle|\Delta B_x|^p\rangle$ vs $\log_{10}\Delta t$ for the first five moments ($p=1,2,\ldots,5$) and the straight lines (the best fit) are drawn to indicate scaling (1). The magnetic field is measured in units of 10 nT here.

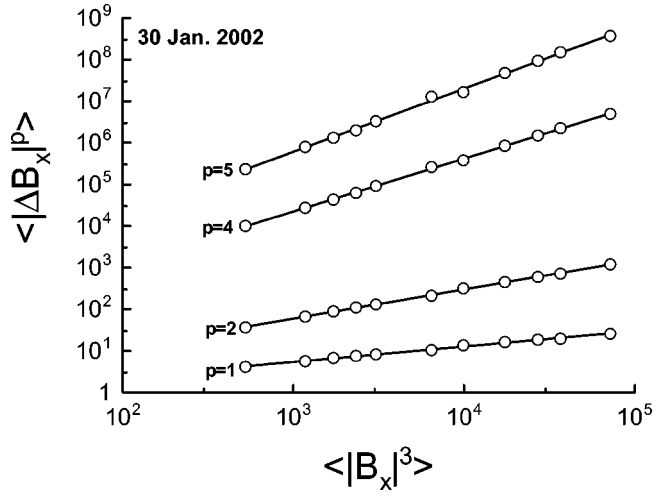

FIG. 3. Extended self-similarity (ESS) representation of the data shown in Fig. 2.

$$\zeta_3 \simeq 1 \tag{3}$$

stemming, in the Kolmogorov theory, from energy conservation under the assumptions of incompressibility, homogeneity, and isotropy (the latter can be relaxed, see, e.g., Ref. [8]). This observation is compatible with Fig. 1. Moreover, Fig. 3 shows the so called extended self-similarity (ESS) of the data (see, for a review, Ref. [16]), when relying on Eq. (3) one uses scale $\langle|\Delta B_x|^3\rangle$ instead of scale Δt. The ESS allows us to make a minor correction of the high moments. Figure 4 shows the corrected intermittency exponents ζ_p versus p (circles). We also show for comparison the intermittency exponents obtained for Kolmogorov fluid turbulence (crosses, of Table 1 Ref. [16]). Thus, one has the Kolmogorov nature not only for one energy spectrum scaling exponent, but for additional five scaling exponents describing the fine intermittency properties of B_x fluctuations.

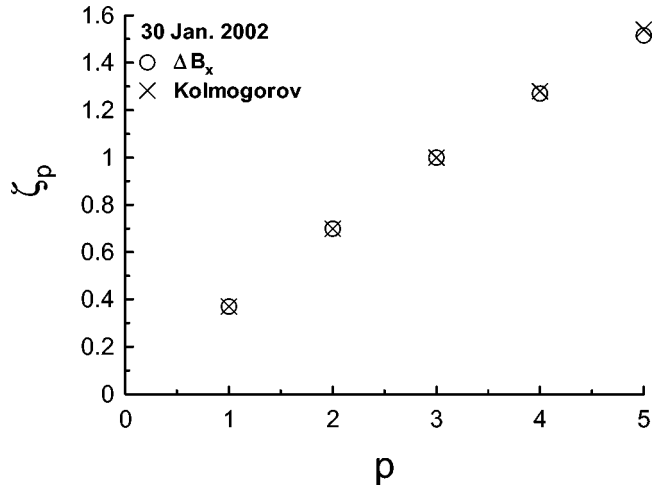

FIG. 4. The intermittency exponents ζ_p versus p (circles). Crosses correspond to the intermittency exponents obtained for Kolmogorov fluid turbulence (Table 1 of Ref. [16]).

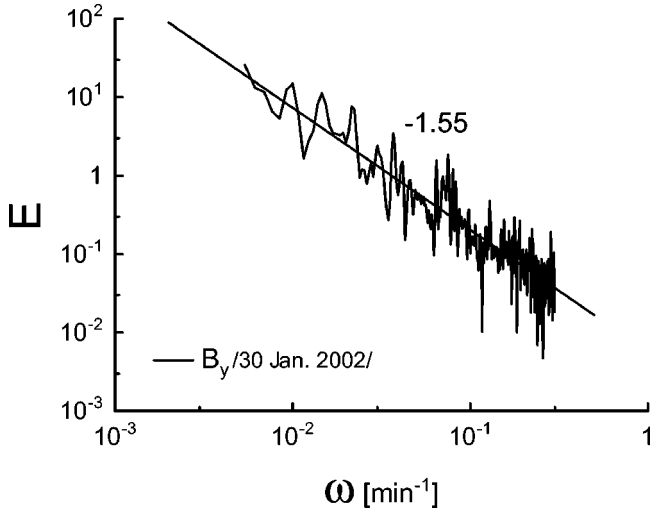

FIG. 5. Energy spectra for the B_y component of the IMF. The straight line (the best fit) is drawn to indicate scaling law dependence (in the log-log scales). The line slope -1.55 ± 0.10 indicates the Iroshnikov scaling $-3/2$.

Now let us turn to the B_y component of the magnetic field. Figure 5 shows energy spectrum for the B_y component. The straight line (the best fit) is drawn to indicate a scaling law dependence (in the log-log scales). The lines slope -1.55 ± 0.10 indicates the Iroshnikov scaling $-3/2$.

The incompressible magnetohydrodynamic equations can be written in the form

$$\partial_t \mathbf{z}^{\pm} + \mathbf{z}^{\mp}\cdot\nabla\mathbf{z}^{\pm} + \nabla p = \nu\Delta\mathbf{z}^{\pm}, \quad \text{div } \mathbf{z}^{\pm} = 0, \tag{4}$$

where $\mathbf{z}^{\pm}$ denote the Elsässer variables $\mathbf{z}^{\pm} = \mathbf{v} \pm \mathbf{B}$. There are good reasons to doubt the unit magnetic Prandtl number assumption for the solar wind [17]. This assumption, however, places no restrictions on our analysis if we consider the in-

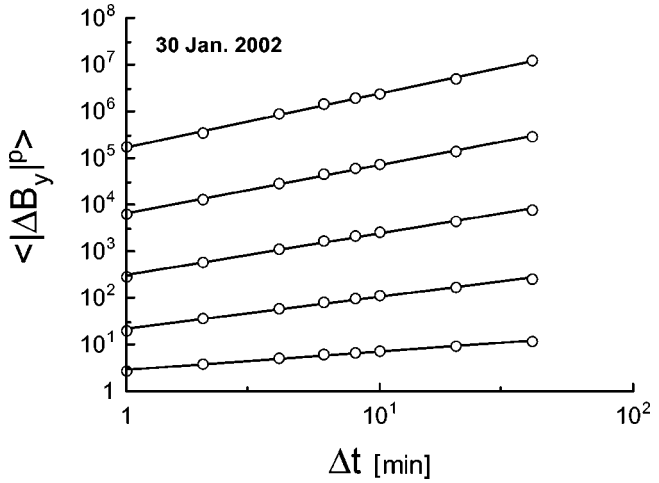

FIG. 6. $\log_{10}\langle|\Delta B_y|^p\rangle$ vs $\log_{10}\Delta t$ for the first five moments ($p = 1,2,\ldots,5$). The straight lines (the best fit) are drawn to indicate scaling (1), but now for the B_y component of the IMF (the magnetic field is measured in units of 10 nT).

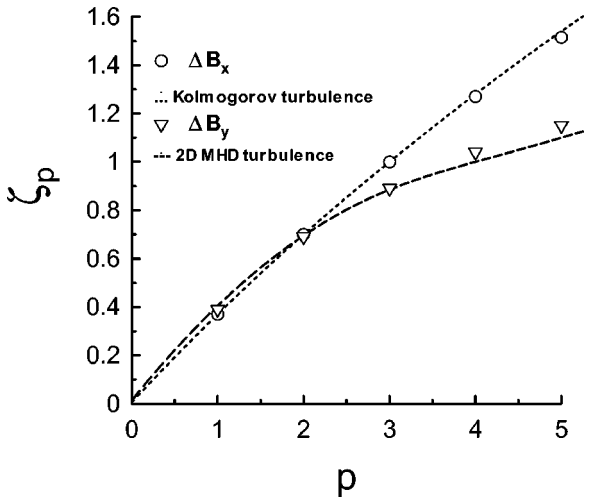

FIG. 7. The intermittency exponents extracted from Fig. 6 (triangles). Circles correspond to the intermittency exponents of the B_x component. The dotted curve corresponds to the Kolmogorov intermittency [16], and the dashed curve corresponds to the data obtained in Ref. [18] for the Elsëser variables in the driven 2D MHD turbulence.

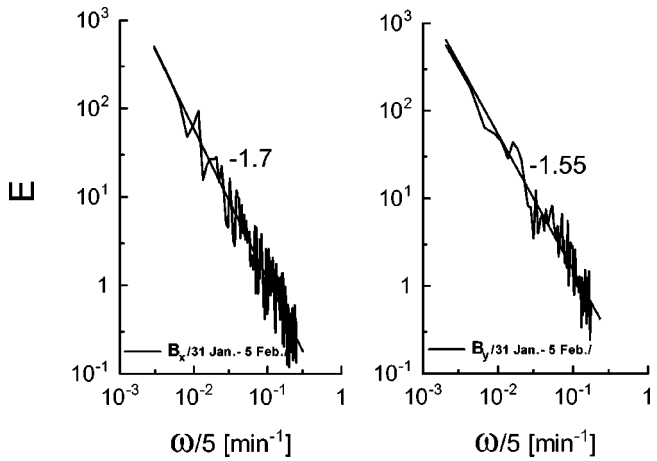

FIG. 8. Energy spectra of the B_x and B_y components of the IMF (measured in nT) for a six-day period: 31 January–5 February 2002. The straight lines (the best fit) are drawn to indicate scaling law dependence (in the log-log scales). The line slope -1.7 ± 0.1 indicates Kolmogorov-like scaling $-5/3$ and the line slope -1.55 ±0.10 indicates the Iroshnikov scaling $-3/2$.

ertial range. To justify the use of the Elsässer variables to interpret the magnetometer data we again need information on the local velocity field (e.g., whether the velocity field was equipartitioned or the extent to which it was aligned), which is not available for us. The absence of measurements of the velocity field **v** makes it quite a leap of faith to test theoretical predictions derived for the Elsässer variables, using measurement of **B** alone.

One of the main differences between hydrodynamic and MHD turbulence is the interaction time τ. In MHD turbulence the interaction time τ is governed by the large-scale magnetic field B_0: $\tau\propto(B_0k)^{-1}$. Small-scale fluctuations behave like Alfvén waves traveling in opposite directions. Assuming that the energy dissipation is proportional to the interaction time τ, dimensional analysis leads to the Iroshnikov scaling $-3/2$ for the energy spectrum (in this situation the energy spectrum is controlled by the Alfvén effect). The same dimensional analysis for structure functions of the Elsëser variables leads to the nonintermittent scaling,

$$\langle|\mathbf{z}^{\pm}(\mathbf{x}+\mathbf{r})-\mathbf{z}^{\pm}(\mathbf{x})|^p\rangle\sim r^{\zeta_p}, \tag{5}$$

with $\zeta_p=p/4$, instead of the nonintermittent Kolmogorov relation $\zeta_p=p/3$. For intermittent case both Kolmogorov and Iroshnikov predictions of the ζ_p behavior are violated. But for ordinary fluid turbulence the particular value $\zeta_3=1$ is still valid, because this is a rigorous consequence of the Navier-Stokes equations. There are arguments that the particular equation $\zeta_4=1$ can be sustained in the intermittent MHD, but no exact relation supporting this assumption still suggested. Though results of a direct numerical simulation of a *driven* 2D MHD turbulence [18] support this statement.

Figure 6 shows $\log_{10}\langle|\Delta B_y|^p\rangle$ versus $\log_{10}\Delta t$ for first five moments ($p=1,2,\ldots,5$) and the straight lines (the best fit) are drawn to indicate scaling (1), but now for B_y component of the magnetic field (the magnetic field is measured in the units 10 nT here). The intermittency exponents extracted from this figure are shown in Fig. 7 as triangles. The previously discussed exponents corresponding to B_x component are also shown (as circles) for comparison. The dotted curve corresponds to the Kolmogorov intermittency [16], and dashed curve corresponds to the numerical simulation data obtained in Ref. [18] for the Elsëser variables in the driven 2D MHD turbulence.

Finally, Fig. 8 shows energy spectra of the B_x and B_y components of the magnetic field fluctuations measured for additional six days: 31 January–5 February 2002. One can see that the picture is similar to those shown in Figs. 1 and 5. It is also worth noting that during all these days the local mean magnetic field was practically perpendicular to the x axis,

$$\frac{[\langle B_y\rangle^2+\langle B_z\rangle^2]^{1/2}}{|\langle B_x\rangle|}\simeq 16$$

(cf. Refs. [19,20] and references therein).

The example of the specific three-dimensional symmetries of solar-wind fluctuations at the libration point given in the present paper can be considered as a complementary one to the two-year IMF ensemble analysis discussed above [3]. This example (''event'') shows a remarkable possibility of combination of the profound Kolmogorov (3D) properties and Alfvén (2D) properties in a single event not only on the spectrum level, but also on the level of fine intermittency. Such an occurrence represents a challenge for modern plasma theory, but seems to be a characteristic part of the solar-wind plasma.

The author is grateful to K.R. Sreenivasan for discussion.

[1] M.L. Goldstein, Astrophys. Space Sci. **227**, 349 (2001).
[2] L.F. Burlaga, *Interplanetary Magnetohydrodynamics* (Oxford University Press, New York, 1995).
[3] W.H. Matthaeus, M.L. Goldstein, and D.A. Roberts, J. Geophys. Res. **95**, 20 673 (1990).
[4] S. Oughton, W.H. Matthaeus, and S. Ghosh, Phys. Plasmas **5**, 4235 (1998).
[5] W.H. Matthaeus, S. Oughton, S. Ghosh, and M. Hossain, Phys. Rev. Lett. **81**, 2056 (1998).
[6] M.L. Goldstein and D.A. Roberts, Phys. Plasmas **6**, 4154 (1999).
[7] D.A. Roberts, M.L. Goldstein, A.E. Deane, and S. Ghosh, Phys. Rev. Lett. **82**, 548 (1999).
[8] A. S. Monin and A. M. Yaglom, *Statistical Fluid Mechanics: Mechanics of Turbulence* (MIT Press, Cambridge, MA, 1975), Vol. 2.
[9] W.H. Matthaeus, M.L. Goldstein and C. Smith, Phys. Rev. Lett. **48**, 1256 (1982).
[10] J.V. Shebalin, W.H. Matthaeus, and D. Montgomery, J. Plasma Phys. **29**, 525 (1983).
[11] D. Montgomery, in *Lecture Notes in Turbulence: Lecture Notes from NCAR-GTP Summer School, June, 1987*, edited by J.R. Herring and J.C. McWilliams (World Scientific, Singapore, 1989), p. 139.
[12] J.W. Bieber, W. Wanner, and W.H. Matthaeus, J. Geophys. Res. **101**, 2511 (1996).
[13] V. Carbone, F. Malara, and p. Veltri, J. Geophys. Res. **100**, 1763 (1995).
[14] S. Ghosh, W.H. Matthaeus, D.A. Roberts, and M.L. Goldstein, J. Geophys. Res. **103**, 23 691 (1998).
[15] M. Ruderman, M.L. Goldstein, D.A. Roberts, and A. Deane, J. Geophys. Res. **104**, 17 057 (1999).
[16] R. Benzi, L. Biferale, S. Coliberto, M.V. Struglia, and R. Tripiccione, Physica D **96**, 162 (1996).
[17] D. Montgomery, J. Geophys. Res. **97**, 4309 (1992).
[18] H. Politano, A. Pouquet, and V. Carbone, Europhys. Lett. **43**, 516 (1998).
[19] P. Goldreich and H. Sridhar, Astrophys. J. **38**, 763 (1995).
[20] J. Cho, A. Lazarian, and H. Yan, e-print astro-ph/0112366.